

DEUTSCHES ELEKTRONEN-SYNCHROTRON **DESY**

DESY 87-010
February 1987



GLUONIUM SPECTRUM IN QCD

by

C.A. Dominguez

Deutsches Elektronen-Synchrotron DESY, Hamburg

ISSN 0418-9833

NOTKESTRASSE 85 · 2 HAMBURG 52

DESY behält sich alle Rechte für den Fall der Schutzrechtserteilung und für die wirtschaftliche Verwertung der in diesem Bericht enthaltenen Informationen vor.

DESY reserves all rights for commercial use of information included in this report, especially in case of filing application for or grant of patents.

**To be sure that your preprints are promptly included in the
HIGH ENERGY PHYSICS INDEX ,
send them to the following address (if possible by air mail) :**

**DESY
Bibliothek
Notkestrasse 85
2 Hamburg 52
Germany**

1. INTRODUCTION AND CONCLUSIONS

GLUONIUM SPECTRUM IN QCD *

C.A. Dominguez **

Deutsches Elektronen-Synchrotron DESY,
D-2000 Hamburg, FRG

ABSTRACT

The scalar (0^{++}) and the tensor (2^{++}) gluonium spectrum is analyzed in the framework of QCD sum rules. Stable eigenvalue solutions, consistent with duality and low energy theorems, are obtained for the mass and width of these glueballs.

* Invited talk at the "International Workshop on Quarks, Gluons and Hadronic Matter". University of Cape Town, February 1987. Based on work done in collaboration with N. Paver.

** Alexander von Humboldt Research Fellow. On leave of absence from: Facultad de Fisica, Pontificia Universidad Católica de Chile, Santiago, Chile.

In the early days of QCD it was recognized /1/ that the existence of bound states of gluons, or glueballs, is a natural consequence of this non-Abelian gauge theory. Since then the problem has been twofold: (i) to make reliable theoretical predictions for the gluonium spectrum, and (ii) to look for clear experimental signatures that would unambiguously identify a glueball. In spite of the impressive progress achieved so far in both fronts these issues are still unsettled.

On the theoretical front, since an exact analytical solution to the bound state problem in QCD remains to be achieved, approximation schemes and model calculations are at present unavoidable. Attempts to estimate the gluonium spectrum along these lines include: (a) numerical simulations of QCD on a lattice /2/, (b) QCD-sum rules /3/, (c) bag models /4/, and a variety of other models /5/. There seems to be a consensus that the lowest lying glueball should be the scalar ($J^{PC} = 0^{++}$) followed by the isoscalar (0^{++}) and the tensor (2^{++}). A notable exception is a recent claim /6/ that the 0^{++} should lie above the 2^{++} . Concerning the masses, most estimates place the scalar glueball at $M_{0^{++}} \simeq 1.0-1.5$ GeV and the tensor at $M_{2^{++}} \simeq 1.5-2.0$ GeV. It should be pointed out, however, that depending on how one translates lattice QCD results into physical units one could find 0^{++} masses as low as $M_{0^{++}} \simeq 600 - 650$ MeV /2.a/. A recent QCD-sum rule analysis /3.d/, to be described here, shows that such a low value for the scalar glueball mass is likely an upper bound. A mass $M_{0^{++}} \simeq 1-1.5$ GeV appears in conflict with the Operator Product Expansion (OPE) and low energy theorems in QCD. Our results confirm an earlier claim by the ITEP group /3.a/ that scalar gluonium should be abnormally light. The expected 0^{++} total width is even more uncertain, as some authors find it small /7/ and others large /3.b/, /5.d/. Our results indicate that the light scalar glueball is very narrow. On the other hand, an analysis of the 2^{++} channel in the same QCD-sum rules framework /3.e/ reveals at least two resonances: $M_1 \simeq 1.6-1.7$ GeV, $\Gamma_1 \simeq 100-150$ MeV, and $M_2 \simeq 2.0-2.1$ GeV,

$\Gamma_2 \approx 200$ MeV.

A very brief (and oversimplified) summary of the experimental situation for 0^{++} and 2^{++} gluonium may be stated as follows. A 0^{++} glueball candidate - G(1590) - was seen through its $\eta\eta'$ decay at the CERN-SPS /8/; however, recent CERN-ISR /9/ results ("ISR gluonium search experiment") show no sign of it. According to an analysis of $\pi\pi$ phase shift data up to $K\bar{K}$ threshold /10/, a scalar glueball could be excluded unless it is very narrow ($\Gamma \approx 2-3$ MeV) or it is broad and lies around 650 MeV where mixing with quark states would make it appear very narrow. A more recent coupled channel analysis /11/ of $I = 0$ S-wave $\pi\pi$ and $K\bar{K}$ final states, which includes the latest CERN-ISR data /9/, reveals three resonances in the 1 GeV region - S_1 (991), S_2 (988), Θ (900) - i.e. one more than expected from the naive quark model. In view of its properties the narrow S_1 (991) state appears to be a serious scalar glueball candidate /11/. However, the existence of a lighter 0^{++} glueball cannot be categorically ruled out provided it is very narrow. Notice that the experimental sweep of the $\pi\pi$ spectrum in the CERN-ISR experiment /9/ is of 10 MeV bins, while earlier high statistics $\pi\pi$ data /12/ have a bin width of 20 MeV. Turning to tensor gluonium, present candidates are: (i) the Θ (1700) first seen in radiative J/ψ decays at SLAC /13/. The latest values of the Θ (1700) parameters are $M_\Theta = 1720 \pm 7$ MeV, $\Gamma_\Theta = 132 \pm 15$ MeV, and $J^{PC} = 2^{++} / 13.b/$. In addition, the CERN-ISR gluonium search experiment has now some evidence for the Θ (1700). (ii) The three $\phi\phi$ resonances g_T (2050), g_T (2300) and g_T (2350), ($\Gamma \approx 200-300$ MeV), seen in $\pi^+\pi^- \rho \rightarrow \phi\phi\eta$ at Brookhaven /14/. There is also some evidence for these states from $J/\psi \rightarrow \gamma\phi\phi$ measured at DCI /15/.

A discussion of the arguments which favour or disfavour a glueball interpretation of all the above candidates is beyond the scope of this talk. The interested reader should consult e.g. /16/ for recent reviews.

In the remainder of this Section I wish to discuss the key results and conclusions of our QCD-sum rule estimate of the mass and width of scalar /3.d/ and tensor gluonium /3.e/. A description of the method and technical details are given in the following Sections.

The gluonium spectrum can be studied in QCD by considering the following two-point function

$$\Pi(q^2) = i \int d^4x e^{iqx} \langle 0 | T (J(x) J(0)) | 0 \rangle, \quad (1)$$

where

$$J(x) = \beta_1 \frac{\alpha_s}{\pi} G_{\mu\nu}^a(x) G_{\mu\nu}^a(x) + \text{quark contributions} \quad (2)$$

is the local current which creates 0^{++} gluonium from the vacuum, and

$$J(x) \longrightarrow J_{\mu\nu}(x) = -G_{\mu\nu}^a(x) G_{\mu\nu}^a(x) + \frac{1}{4} \frac{g}{\partial_{\mu\nu}} G_{\mu\nu}^a(x) \partial_{\mu\nu} \text{quark contributions} \quad (3)$$

has 2^{++} gluonium quantum numbers. The current (2) is proportional to the trace of the energy-momentum tensor $\Theta_{\mu\nu}(x)$, and (3) is just $\Theta_{\mu\nu}(x)$. The key assumption behind the whole ITEP program /3.a/ is the validity of the OPE even in the presence of non-perturbative effects. These are parametrized by non-vanishing vacuum expectation values of quark and gluon fields (vacuum condensates) of increasing dimensionality which introduce power corrections to asymptotic freedom. A relation between these vacuum condensates and resonance parameters follows immediately from analyticity. Depending on the choice of weight in the dispersion relation one may obtain e.g. Hilbert transform -, Laplace transform -, Gaussian transform -, or Finite Energy - QCD sum rules. A comparative descrip-

tion of these QCD sum rules may be found in Section 2. The following results, however, are essentially independent of the type of sum rule used in the analysis.

A. Scalar Gluonium

A simple relation between the mass of scalar gluonium and the vacuum condensates, which approximately summarizes more refined expressions from Laplace and Gaussian transform - as well as Finite Energy - QCD sum rules, may be written as

$$M_{0^{++}}^2 \simeq \frac{C_6 \langle O_6 \rangle}{\Pi(0)}, \quad (M_{0^{++}} > 2\mu\pi) \quad (4)$$

valid within a factor of 2. In (4) $C_6 \langle O_6 \rangle$ is a short notation for the triple-gluon condensate

$$C_6 \langle O_6 \rangle = 2 \frac{\beta_1^2}{\pi^2} \left(\frac{\alpha_s}{\pi} \right) \langle O_6 \rangle = 2 \frac{\beta_1^2}{\pi^2} \langle O_6 \rangle = 2 \frac{\beta_1^2}{\pi^2} f^{abc} \int \epsilon_{\mu\nu}^a \epsilon_{\nu\rho}^b \epsilon_{\rho\mu}^c \langle O_6 \rangle, \quad (5)$$

and $\Pi(0)$ is the $Q^2 = 0$ value of (1) with $J(x)$ given by (2). The total width is approximately given by

$$\Gamma_{0^{++}} \simeq \frac{3}{2\pi} M_{0^{++}}^5 \times (\text{phase space}), \quad (6)$$

which is a very good approximation (within 10 %) to more refined results. Before discussing numbers a few remarks on Eqs. (4) and (6) are in order:

- (i) Notice that the mass scale in this channel is set by non-perturbative effects rather than by asymptotic freedom as e.g. for ordinary vector mesons or tensor gluonium (see below). This fact was first recognized by the ITEP group

/3.a/. However, such a situation is not novel, viz. it is well known that the nucleon mass scale is set by the quark vacuum condensate /17/

$$M_N \simeq \text{Const.} \times |\langle O_3 \rangle|^{1/3} \simeq 1 \text{ GeV}. \quad (7)$$

The reason for such a behaviour of the 0^{++} channel is easy to see from the diagrammatic representation of the OPE shown in Fig. 1. Purely perturbative effects

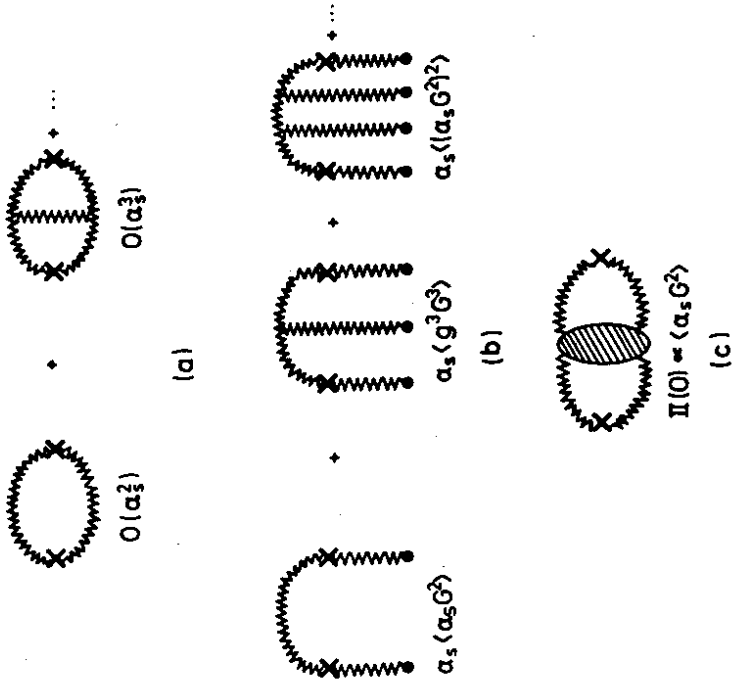


Fig. 1

- (Fig. 1-a) start at order $O(\Lambda_s^2)$ and thus are suppressed relative to a) the non-perturbative gluon condensate contributions which are only of order $O(\Lambda_s^3)$ (Fig. 1-b), and relative to $\Pi(0)$ which is of order $O(1)$ (Fig. 1-c). Numerically,

asymptotic freedom begins to become important at $S_0 > 7 \text{ GeV}^2$. Clearly, at such high energies one could hardly invoke duality. In other words, a hadronic parametrization of the spectral function valid up to such a threshold does not seem feasible or even meaningful.

(ii) The simple formulas (4) and (6) are obtained from all the various versions of QCD-sum rules after neglecting perturbative and continuum contributions, $C_4 \langle O_4 \rangle$ relative to $II(0)$, and the remaining non-leading gluon condensates. Of all these contributions the continuum is the most important; it may become numerically comparable to $C_6 \langle O_6 \rangle$ and thus Eq. (4) is valid within a factor of 2. This approximation, though, has only a minor impact on the total width (6).

(iii) The approximations (4) and (6) are for pure gluodynamics in the QCD sector. However, as first pointed out in /3.b/, quark contributions to this sector do not play any important role in the determination of the mass and total width of the glueball. Notice that for $q = u, d, s$ these effects are suppressed by factors of $\alpha_s^2 \kappa_q^2 / q^2$. For heavier flavors the leading non-perturbative contributions vanish on account of $\langle \bar{c}c \rangle = \langle \bar{b}b \rangle = \dots = 0$. Quark effects have been effectively taken into account in the parametrization of the spectral function, where we have included the appropriate $\bar{K}K$, $K\bar{K}$, and $\eta\eta$ intermediate state contributions. Up to moderate widths ($\Gamma \lesssim M/2$), though, phase space effects tend to cancel in the mass, and affect the width mostly for mass values very close to the two-pseudoscalar-meson thresholds.

The crucial quantity having the biggest impact on the 0^{++} glueball mass and width is $II(0)$. Using Ward identities and commutation relations for the energy-momentum tensor the IIEP group derived the following low energy theorem /3.a/

$$II(0) = -16 \beta_1 \langle 0 | \frac{\alpha_s}{\pi} G_{\mu\nu}^a G_{\mu\nu}^a | 0 \rangle. \quad (8)$$

A discussion of the numerical values of the gluon condensates may be found in Section 3. Let me just point out now that after allowing for very conservative errors in these condensates, of up to factors of 10!, plus the factor of two uncertainty in (4) one finds

$$M_{0^{++}} \simeq 300 - 650 \text{ MeV}, \quad (9)$$

$$\Gamma_{0^{++}} \simeq 1 - 50 \text{ MeV}. \quad (10)$$

These results are confirmed by a more careful analysis based on the complete expressions for M and Γ which follow from the various versions of QCD-sum rules (See Section 3). The uncertainties allowed in the gluon condensates to obtain (9)-(10) have been grossly exaggerated. Using the best available estimates one would find instead

$$M_{0^{++}} \simeq 350 - 550 \text{ MeV}, \quad (11)$$

$$\Gamma_{0^{++}} \simeq 1 - 10 \text{ MeV}. \quad (12)$$

My intention has been to show that even a gross exaggeration of the uncertainties yields a 0^{++} mass well below 1 GeV. In fact, one can easily turn the problem around and ask for the values of the condensates which would yield a 1-1.5 GeV scalar glueball. The problem is a bit more complicated than explained so far, as one has to look also for the implications on the values of higher dimensional condensates, chiefly $C_8 \langle O_8 \rangle$ (See Section 3), but the answer is well outside reasonable limits. Additional non-perturbative effects not accounted for in the OPE (direct instantons?) could, in principle, offer an escape route to evade such a light scalar glueball. However, at the present time this possibility is only a speculation. Let me reiterate in closing that given the present experimental binning of the $\bar{K}K$ spectrum it is not possible to rule out categorically a light 0^{++} glueball of a few MeV width.

B. Tensor Gluonium

In the language of the OPE the mass scale for tensor gluonium is expected to be rather different from that for scalar gluonium /3.a/. This may be easily seen from Fig. 2 which shows the lowest order perturbative contribution, of order

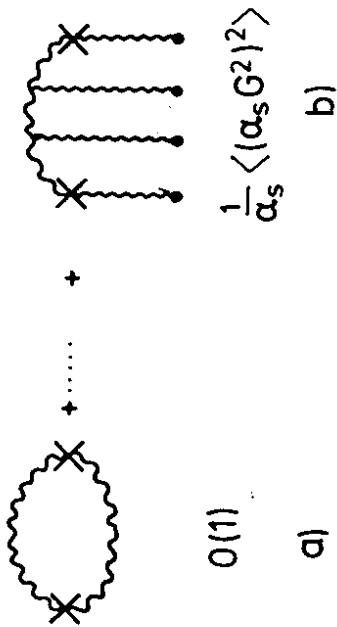


Fig. 2

$O(1)$, and the leading non-perturbative term $C_g \langle O_g \rangle$ (there are no corrections of dimension 4 and 6 in this channel /3.a/). One expects then the scale to be set by asymptotic freedom with small power corrections due to the gluon condensates of dimension 8, 10, etc. Notice that although the Wilson coefficient in $C_g \langle O_g \rangle$ is of order $O(1/\alpha_s)$ the whole term is still numerically small. This contrasts with the 0^{++} channel where asymptotic freedom played essentially no role and the scale was set by the gluon condensates.

Using a finite-width parametrization of the spectral function, with tensor glueball couplings to $\pi\pi$, $K\bar{K}$ and $\eta\eta$, in the framework of the FESR we find (See Section 4).

$$M_{2^{++}} \simeq 1.6 - 2.0 \text{ GeV}, \tag{13}$$

$$\Gamma_{2^{++}} \simeq 100 - 200 \text{ MeV}, \tag{14}$$

in line with earlier Laplace transform QCD-sum rule estimates in zero-width /3.a,c,f/. However, the eigenvalue problem posed by the FESR turns out to be unstable signaling the need for additional resonances in the spectral function. This is similar to what happens in the ρ -channel /19/. Adding a second resonance, even if done in the most economical fashion, clearly reduces the predictive power of the sum rules. Nevertheless, our experience from the ρ -channel indicates that in the process of stabilizing the eigenvalue problem one can make a reasonable semi-quantitative guess of the shape of the spectral function. Using this example as guidance one may assume that the location of the 2^{++} ground state is not affected substantially by the addition of excitations and then search for the resonance parameters which stabilize the eigenvalue problem. In this way we find

$$M_1(2^{++}) \simeq 1.7 \text{ GeV}, \quad \Gamma_1(2^{++}) \simeq 150 \text{ MeV}, \tag{15}$$

$$M_2(2^{++}) \simeq 2 - 2.2 \text{ GeV}, \quad \Gamma_2(2^{++}) \simeq 200 \text{ MeV}, \tag{16}$$

which shows that the θ (1700) and at least one of the $g_1(2000)$ glueball candidates can be easily accounted for in QCD.

2. THEORETICAL FRAMEWORK: QCD-SUM RULES

In this Section I discuss the main ideas behind the QCD-sum rule programme introduced by Shifman, Vainshtein and Zakharov /19/. The presentation is intended for non-specialists in this field and thus rigor will be sacrificed for the sake of clarity.

2.A The various versions of QCD-sum rules

Let me begin by recalling the two well known realizations of QCD: (i) at short distances one has the asymptotic freedom property of QCD which allows for the performance of reliable perturbative calculations and, in principle, to any desired order in the strong interaction running coupling constant $\alpha_s(Q^2)$, $\alpha_s(Q^2) \sim 1/\ln(Q^2/\Lambda^2)$. (ii) At the other end, i.e. at low energies, QCD is realized through the non-linear σ -model, chiral lagrangians, etc. Reliable calculations are also possible here by means of chiral perturbation theory and, again in principle, to any number of loops. If QCD is the correct theory for the strong interactions then there should exist an intermediate region where both realizations overlap and coexist. The ITEP programme approaches this region from the short distance domain introducing in the way power corrections to asymptotic freedom which arise from non-perturbative effects. These power corrections are expected to be more important than higher order radiative corrections as illustrated by the following example /19/: The β - A_1 mass splitting is zero to all orders in perturbation theory.

To see the appearance of these power corrections let us concentrate on the two-point function (1) and consider the OPE

$$i \int d^4x e^{iqx} T(J(x) J(0)) = C_0 \mathbb{1} + \sum_N C_N(q) \hat{O}_N, \quad (17)$$

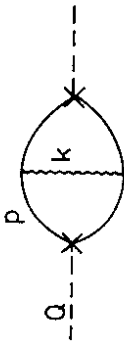
where the Wilson coefficients $C_N(q)$ in this expansion depend on the Lorentz indices and quantum numbers of $J(x)$ and of the local gauge invariant operators \hat{O}_N built from the quark and gluon fields of QCD. These operators are ordered by increasing dimensionality and the Wilson coefficients fall off by corresponding powers of q^2 . The unit operator in (17) has dimension $d=0$ and $C_0 \mathbb{1}$ stands for the purely perturbative contributions. Examples of $d=4$ operators are: $m_q \bar{q}q$, $G_{\mu\nu}^a G^{\mu\nu a}$. In order to use the OPE (17) in (1) one needs to go beyond per-

turbation theory as otherwise $\langle 0 | \hat{O}_N | 0 \rangle$ would vanish identically. The key assumption behind the ITEP programme is that the OPE continues to make sense even in the presence of non-perturbative effects, i.e. the state $|0\rangle$ in (1) is identified with the physical vacuum. At our present stage of understanding of QCD it is not possible to compute these vacuum condensates from first principles. They remain as phenomenological parameters to be fixed e.g. by relating them to experiment through dispersion relations or by numerical simulations of QCD on a lattice. The Wilson coefficients, though, obey renormalization group equations and are calculable in perturbation theory.

An intuitive picture of what has been stated above is provided by the following example /3.a/. Consider a local current built from light quark fields $J(x) = \bar{q}(x)q(x)$, insert it in the two-point function (1), and look at the first non-trivial graph, Fig. 3.a, in the limit of large incoming momentum Q . When all internal momenta are also large this graph effectively reduces to a point (Fig. 3b) and this contribution may be computed in perturbation theory. However, in performing the loop integrations one will inevitably hit a region where e.g. k is small (soft gluon) and the quark momenta are all large. In such a region one expects the gluon propagator to be modified by non-perturbative effects and the graph effectively reduces to the one shown in Fig. 3.c. The non-perturbative fluctuation in this case is nothing but the gluon condensate $\langle 0 | G_{\mu\nu}^a G_{\mu\nu}^a | 0 \rangle$ times a coefficient absorbing hard momenta and thus calculable in perturbation theory. If, instead, the gluon is hard and some of the quark lines are soft one gets e.g. the four-quark vacuum condensate. This factorization of short and long distance effects is of course what the OPE is all about.

Once the validity of the OPE beyond perturbation theory is assumed the rest follows immediately from analyticity, viz the two-point function (1) satisfies the dispersion relation ($q^2 \rightarrow -q^2$, q^2 space-like)

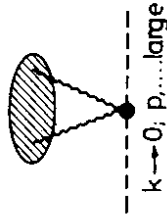
$$\Pi(Q^2) = \frac{1}{\pi} \int_0^\infty ds \frac{\text{Im} \Pi(s)}{s + Q^2} + \text{subtractions}, \quad (18)$$



(a)



(b)



(c)

Fig.3

defined up to a number \underline{n} of subtraction constants. One may get rid of these subtractions by taking an appropriate number of derivatives in (18). This yields the power moments or Hilbert-transform sum rules

$$M_n(Q^2) \equiv \frac{1}{n!} \left(-\frac{d}{dQ^2} \right)^n \Pi(Q^2) = \frac{1}{\pi} \int_0^\infty ds \frac{\text{Im} \Pi(s)}{(s + Q^2)^{n+1}}, \quad (19)$$

with $n = d+1$, where d is the asymptotic behaviour in s of the spectral function $\frac{1}{\pi} \text{Im} \Pi(s)$. Up to the values of the vacuum condensates the l.h.s. of (19)

can be computed in QCD through the OPE (17), i.e.

$$M_n(Q^2) \Big|_{\text{QCD}} = \frac{1}{n!} \frac{C_0}{Q^2} \left[1 + \sum_{p=2}^P \frac{F}{(Q^2)^p} C_{2p} \langle \hat{O}_{2p} \rangle \right]. \quad (20)$$

This result will of course make sense only for values of Q^2 such that the power corrections remain as corrections. The spectral function appearing in the r.h.s. of (19) may be extracted from experimental data, in which case one could estimate the leading vacuum condensates, or it may be parametrized at low energies by some resonance model; if the condensates are known this provides an estimate of the masses and couplings entering the spectral function. Notice that the high energy behavior of $\text{Im} \Pi(s)$ is calculable in QCD through perturbation theory. The onset of asymptotic freedom is characterized by some threshold S_0 and thus one can approximately write

$$\frac{1}{\pi} \text{Im} \Pi(s) = \frac{1}{\pi} \text{Im} \Pi(s) \Big|_{\text{Res.}} + \theta(s - S_0) \frac{1}{\pi} \text{Im} \bar{\Pi}(s) \Big|_{\text{A.F.}} \quad (21)$$

The sum rules (19) may be regarded as a global duality relation in the sense that the weighted average of the hadronic spectral function for sufficiently large Q^2 should match the theoretical QCD expression for $M_n(Q^2)$. One should keep in mind, though, that in practice the amount of available QCD and hadronic information is limited. The former is restricted to the first few leading power corrections in the OPE, while the latter is usually limited to the ground state resonance or at most its first excitation. This means that the Hilbert-transform (19) may not be the ideal sum rule to carry out this programme. One optimization is obtained by applying to both sides of (19) the operator $/\pi$

$$\hat{L} \equiv \lim_{\substack{N \rightarrow \infty \\ Q^2 \rightarrow \infty}} \frac{(-)^N}{(N-1)!} (Q^2)^N \frac{d^N}{(dQ^2)^N} \quad (22)$$

This procedure leads to the Laplace-transform sum rules of SVZ /19/

$$\begin{aligned} M(\sigma) &\equiv \frac{G_0}{\sigma^N} \left[1 + \sum_{p=2}^{\infty} \frac{1}{(p-1)!} G_{2p} \langle \hat{O}_{2p} \rangle \sigma^p \right] \\ &= \frac{1}{\pi} \int_0^{\infty} ds e^{-s\sigma} \text{Im} \Pi(s). \end{aligned} \quad (23)$$

In this limiting process a transmutation of the variable $1/Q^2$ into σ has occurred, so that now the non-perturbative effects appear as power corrections in the new short distance variable σ . The sum rules (23) may be regarded as an improvement over the Hilbert-transform sum rules in the sense that because of the exponential factor the r.h.s. of (23), at moderate values of σ , is now more sensitive to the low energy behaviour of the spectral function. At the same time, higher dimensional vacuum condensates become factorially suppressed, a welcomed feature.

Another optimization is obtained by applying to both sides of (23) the operator /20/

$$\hat{L} \equiv \lim_{\substack{\sigma^2 \rightarrow \infty \\ N \rightarrow \infty}} \frac{(-)^N}{(N-1)!} (\sigma^2)^N \frac{d^N}{(d\sigma^2)^N}, \quad (24)$$

$$\left. \frac{\sigma^2}{N} \right|_{\sigma^2 = \frac{1}{N}} = \frac{1}{N}$$

yielding the Gauss-Weierstrass sum rules of Bertlmann, Launer and de Rafael /20/

$$\begin{aligned} G(\hat{s}, \tau) &= \frac{1}{\sqrt{\pi}} 2^{n/2} \tau^{(n-1)/2} G_0 \left[e^{-\hat{s}^2/8\tau} D_{-n}(-\hat{s}/\sqrt{2\tau}) \right. \\ &+ \sum_{p=2}^{\infty} \frac{1}{(p-1)!} G_{2p} \langle \hat{O}_{2p} \rangle \frac{e^{-\hat{s}^2/8\tau}}{(\sqrt{2\tau})^p} D_{p-n}(-\hat{s}/\sqrt{2\tau}) \left. \right] \\ &= \frac{1}{\sqrt{4\pi\tau}} \int_0^{\infty} ds \exp\left[-\frac{(s-\hat{s})^2}{4\tau}\right] \frac{1}{\pi} \text{Im} \Pi(s), \end{aligned} \quad (25)$$

where $D_n(z)$ is the parabolic cylinder function, and the new short distance expansion parameter is proportional to $1/\sqrt{\tau}$. The transform $G(\hat{s}, \tau)$ is just the convolution of the spectral function with a Gaussian centered at an arbitrary point \hat{s} with a finite-width resolution $\sqrt{4\tau}$. The Gauss-Weierstrass transform calculated via QCD is dual to the hadronic spectral function in the sense that the more one knows about QCD the sharper one can take the Gaussians (i.e. τ smaller) and the more accurately the calculated $G(\hat{s}, \tau)$ should approximate the physical spectrum. If the QCD bound state problem would be completely solved then one could take $\tau = 0$. In this hypothetical case

$$G(\hat{s}, 0) = \frac{1}{\pi} \text{Im} \Pi(\hat{s}), \quad (26)$$

and one would have strict local duality. In practice, however, due to the limited amount of QCD information τ must be kept finite, typically $\tau \approx 0.5 - 1 \text{ GeV}^2$.

There is a very interesting and useful analogy between Gaussian sum rules and the theory of the heat equation which allows for a quantitative definition of duality in QCD /20/. This analogy is based on the observation that $G(\hat{s}, \tau)$ obeys the partial differential equation

$$\frac{\partial^2 G(s, \tau)}{(\partial s)^2} = \frac{\partial G(s, \tau)}{\partial \tau}, \quad (27)$$

which is the one-dimensional heat equation if one reinterprets s as a "position" variable and τ as a "time" variable. In this analogy the hadronic spectral function $\frac{1}{\pi} \text{Im} \Pi(s)$ represents the initial heat distribution in a semi-infinite rod $0 \leq s \leq \infty$ and $G(s, \tau)$ measures the evolution in "time" of the heat distribution in this rod. This provides a very convenient framework to check the consistency between a given phenomenological ansatz (or data) for the spectral function and a specific choice of vacuum condensates. In fact, after a time τ sufficiently large so that the uncalculated QCD corrections become relatively small, the predicted QCD heat distribution should match the evolution of the phenomenological ansatz (or data). This is the heat evolution test proposed by BLR /20/, and which serves as a quantitative formulation of the idea of local duality. In Fig. 4 we show schematically the evolution in "time" of an initial heat distribution (21) when $(1/\pi) \text{Im} \Pi(s)|_{\Lambda_F}$ is approximated by a delta function and $(1/\pi) \text{Im} \Pi(s)|_{\Lambda_F} \approx \text{constant}$ (solid lines). The broken curves in Fig. 4 show the evolution of the QCD heat distribution. In this case there is duality between the low energy parameters and the values of the condensates used to compute the two-point function in QCD. Changing the values of these condensates could destroy duality; this will be signaled by a mismatch between the QCD and the hadronic heat evolutions after a reasonable long "time" has elapsed.

It is possible to obtain still another type of QCD sum rules by writing Hermite moments of the Gauss-Weierstrass transforms. This leads to the so called Finite Energy sum rules (FESR) which e.g. for the current (2) appropriate for scalar gluonium read /3.d/

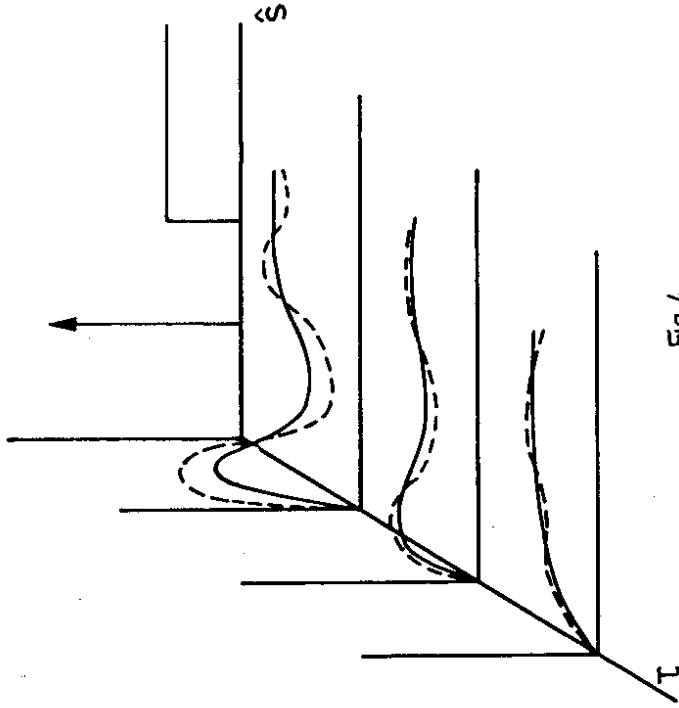


Fig.4

$$\frac{1}{2} C_0 S_0^2 + \Pi(0) - C_4 \langle O_4 \rangle = \frac{1}{\pi} \int_0^{S_0} ds \frac{\text{Im} \Pi(s)}{s}, \quad (28)$$

$$\frac{1}{3} C_0 S_0^3 + C_6 \langle O_6 \rangle = \frac{1}{\pi} \int_0^{S_0} ds \text{Im} \Pi(s), \quad (29)$$

$$\frac{1}{4} C_0 S_0^4 - C_8 \langle O_8 \rangle = \frac{1}{\pi} \int_0^{S_0} ds s \text{Im} \Pi(s), \quad (30)$$

and so on. In these equations C_0 is a perturbative coefficient from the gluonic loop Fig. 1.a, $C_N \langle O_N \rangle$ are related to the gluon condensates, Fig. 1.b, and $\Pi(\omega)$ is a subtraction constant, Fig. 1.c. The integral cutoff S_0 is the threshold for asymptotic freedom which can be predicted as a solution to the above eigenvalue problem. An advantage of the FESR is that the vacuum condensates obey uncoupled eigenvalue equations, in contrast to the Hilbert, Laplace and Gaussian transforms where they appear correlated. However, since S_0 is expected to lie at the border of the resonance region the FESR weigh more the high energy domain and this may call for a more accurate hadronic parametrization. This is not necessarily a handicap, though, as FESR may provide valuable information on excited states.

2.B From QCD-sum rules to predictions

Let us consider any of the QCD-sum rules discussed so far and say we wish to estimate the mass and width of a resonance knowing beforehand the values of the relevant leading vacuum condensates. The first step is to write the spectral function (21). The second term in Eq. (21) offers no problem, at least in principle, as it may be computed in perturbative QCD. As for the resonance piece, the most trivial procedure is to parametrize it by a delta function (zero-width resonance model). However, this two-parameter ansatz (mass and coupling constant) is too crude and may lead to troubles. A more realistic finite-width parametrization can be achieved in some cases by using the information provided by the effective chiral Lagrangian realization of QCD at long distances. For applications of this idea to QCD-sum rules see /21/, /3.d.e/. In any case, a more serious potential problem is that the resonance parameters entering the spectral function depend on the short distance variables: $1/Q^2$ in the Hilbert transform (21), σ in the Laplace transform (23), or $1/\sqrt{s}$ in the Gaussian transform (25). Also, these resonance parameters depend on the threshold for asymptotic freedom, S_0 , in all sum rules including FESR. Obviously these functional dependences are

spurious and, therefore, some criteria are needed before making predictions. Concentrating on the Laplace transform (23) and the FESR e.g. (28)-(30) these criteria are as follows. (a) Laplace transforms: These sum rules do not fix the threshold S_0 which must be guessed e.g. by assuming it to lie somewhere after the ground state and the first excitation (or beyond). To this extent the Laplace sum rules do not provide by themselves a quantitative formulation of local duality. In any case, once S_0 is fixed, predictions for resonance parameters expected to be dual to a given QCD information follow from the criterion that there should exist some region or "window" in σ such that ordinary perturbative QCD remains valid and, at the same time, only the leading power corrections are required /19/. Lacking a quantitative formulation of local duality, a complementary consistency check of the expectation that the resonance parameters so determined are in fact dual to the input QCD information should be performed e.g. by using the heat evolution test of BLR /20/. Experience indicates that this check may lead to surprises /18/, /20/. (b) Finite Energy Sum Rules: The FESR, e.g. (28)-(30) pose a well defined eigenvalue problem whose solutions are the resonance parameters in $\text{Im } \Pi(s)$ as well as S_0 . This may not be enough, however, as this eigenvalue problem may be unstable in the sense that small changes in S_0 could induce large variations in the resonance parameters; clearly an undesirable situation. Such an instability is usually due to an inaccurate parametrization of the spectral function. The following principle due to Pich and de Rafael /21.d/ should be implemented: "Trust FESR only if they are stable in S_0 , only then there exists duality". To be more specific let us consider the ratio of the FESR (28) and

$$\frac{1 + \frac{3 \langle \bar{q}q \rangle}{C_0 S_0^3}}{1 + \frac{2 [\Pi(0) - C_4 \langle O_4 \rangle]}{C_0 S_0^2}} = \left(\frac{3}{2S_0} \right) \frac{\int_{S_0}^{S_0} ds \text{Im } \Pi(s)}{\int_{S_0}^{S_0} \frac{ds}{s} \text{Im } \Pi(s)} \quad (29)$$

The QCD l.h.s. of (31) is shown schematically in Fig. 5 (vertical lines) at some

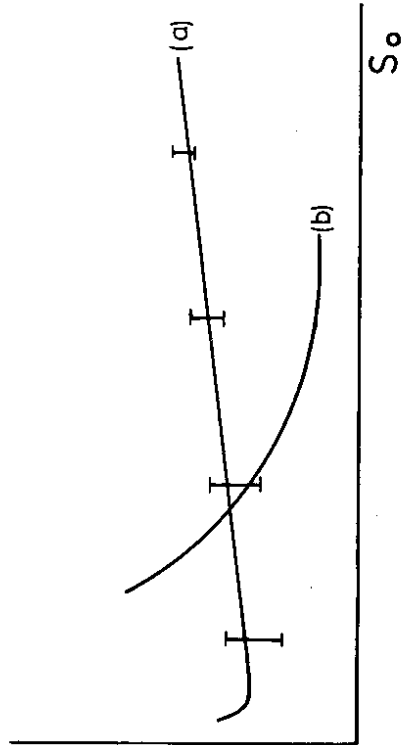


Fig.5

values of S_0 ; the error bars reflect uncertainties in the vacuum condensate parameters. The solid curve (a) shows the schematic behaviour of the hadronic r.h.s. of (31) in a case where the eigenvalue problem is stable, i.e. there is a wide "duality region" within which the resonance parameters in $\text{Im II}(s)$ are dual to QCD. In contrast, the solid curve (b) would correspond to an unstable eigenvalue problem. Additional information would be required in the spectral function in order to stabilize the ratio (31).

3. SCALAR GLUONIUM

3.A The two-point function $\text{II}(Q^2)$ in QCD

The two-point function (1) with $J(x)$ given by (2) reads /3.a/

$$\begin{aligned} \text{II}(Q^2) = & C_0 Q^4 \left(-\frac{1}{\epsilon} - \ln \frac{Q^2}{\mu^2} + 2 \right) + C_4 \langle O_4 \rangle \\ & + \frac{C_6 \langle O_6 \rangle}{Q^2} + \frac{C_8 \langle O_8 \rangle}{Q^4} + \dots, \end{aligned} \quad (32)$$

where

$$C_0 = 2 \left(\frac{\beta_1}{\pi} \right)^2 \cdot \left(\frac{\alpha_s}{\pi} \right)^2, \quad (33)$$

$$C_4 \langle O_4 \rangle = 4 \beta_1^2 \left(\frac{\alpha_s}{\pi} \right) \langle \frac{\alpha_s}{\pi} \zeta_{FUV}^a \zeta_{FUV}^a \rangle, \quad (34)$$

$$C_6 \langle O_6 \rangle = 8 \beta_1^2 \left(\frac{\alpha_s}{\pi} \right)^2 \langle g_s f_{abc} \zeta_{FUV}^a \zeta_{FUV}^b \zeta_{FUV}^c \rangle, \quad (35)$$

$$\begin{aligned} C_8 \langle O_8 \rangle = & 8\pi \left(\frac{\beta_1}{\pi} \right)^2 \alpha_s^3 \left[14 \langle (f_{abc} \zeta_{FUV}^a \zeta_{FUV}^b \zeta_{FUV}^c)^2 \rangle \right. \\ & \left. - \langle (f_{abc} \zeta_{FUV}^a \zeta_{FUV}^b \zeta_{FUV}^c)^2 \rangle \right], \end{aligned} \quad (36)$$

and we have neglected small quark contributions /3.b/. To leading order in α_s the perturbative QCD asymptotic behaviour of the spectral function is

$$\frac{1}{\pi} \text{Im II}(s) \Big|_{\text{A.F.}} \sim C_0 s^2, \quad (37)$$

implying that three subtractions will be required in the dispersion relation.

Subtracting at $Q^2 = 0$ one may write

$$\Pi_R(Q^2) = \Pi(Q^2) - \Pi(0) - Q^2 \Pi'(0) - \frac{1}{2} Q^4 \Pi''(0). \quad (38)$$

Since $\Pi(0)$ is known from the low energy theorem /3.a/

$$\Pi(0) = -16\beta_1 \langle \frac{\alpha_s}{\pi} G_{\mu\nu}^a G_{\mu\nu}^a \rangle, \quad (39)$$

one can make use of this information by writing a dispersion relation for the second derivative of $\Pi_R(Q^2)/Q^2$.

I discuss next the numerical values of the QCD parameters (33)-(36) and (39). Since perturbative contributions will turn out to play a negligible role in this channel we work to leading order in α_s and neglect the Q^2 -dependence of the running coupling constant. With $\beta_1 = -11/2 + n_f/3$ we freeze $\alpha_s(Q^2)$ at its value at $Q^2 = 1 \text{ GeV}^2$, i.e.

$$\frac{\alpha_s}{\pi} \simeq 0.1, \quad (40)$$

in which case

$$C_0 \simeq 0.04. \quad (41)$$

The so called "standard value" of the gluon condensate, as first estimated by SVZ /19/, is

$$\frac{\pi}{3} \langle \alpha_s G^2 \rangle \Big|_{\text{SVZ}} \simeq 0.04 \text{ GeV}^4, \quad (42)$$

leading to

$$C_4 \langle O_4 \rangle \simeq 0.0985 \text{ GeV}^4, \quad (43)$$

$$\text{II}(0) \simeq 0.875 \text{ GeV}^4. \quad (44)$$

However, a recent determination of the gluon condensate shows that (42) is an underestimate by a factor of two to five /18.a,b/. Details of this determination, and a complete list of references to earlier related work, are given in my second contribution to this Workshop /18.c/. In view of this we shall also consider the value

$$\frac{\pi}{3} \langle \alpha_s G^2 \rangle \simeq 0.12 \text{ GeV}^4, \quad (45)$$

with $C_4 \langle O_4 \rangle$ and $\text{II}(0)$ increased accordingly. Concerning the dimension-six triple-gluon condensate, its value is rather uncertain, to wit. A dilute instanton gas (DIGA) calculation gives /3.a/

$$\langle g_s G^3 \rangle \Big|_{\text{DIGA}} = \frac{12}{5} \rho_c^{-2} \langle G^2 \rangle \simeq 0.012 \text{ GeV}^6 \quad (46)$$

where $\alpha_s/\pi \simeq 0.1$, $\rho_c \simeq (200 \text{ MeV})^{-1}$, and (42) have been used. The estimate (46) implies

$$C_6 \langle O_6 \rangle \Big|_{\text{DIGA}} \simeq 0.019 \text{ GeV}^6. \quad (47)$$

On the other hand, a value of the infrared cutoff $\rho_c \simeq (500-600 \text{ MeV})^{-1}$ has been advocated in /22/. This implies

$$C_6 \langle O_6 \rangle \simeq (0.12 - 0.17) \text{ GeV}^6. \quad (48)$$

While in agreement with some phenomenological determinations /23/, (46) disagrees

in sign and magnitude with the result of a modified DIGA (MDIGA) calculation /24/, viz

$$\langle g_s G^3 \rangle \Big|_{\text{MDIGA}} \simeq -0.07 \text{ GeV}^6, \quad (49)$$

which implies

$$C_6 \langle O_6 \rangle \Big|_{\text{MDIGA}} \simeq -0.11 \text{ GeV}^6. \quad (50)$$

Finally, lattice calculations give /25/

$$\langle g_s G^3 \rangle \Big|_{\text{Lattice}} \simeq (6.6 \pm 1.4) \langle \frac{\alpha_s}{\pi} G^2 \rangle^{3/2}, \quad (51)$$

which yields

$$C_6 \langle O_6 \rangle \simeq 0.01 \text{ GeV}^6, \quad (52)$$

if the "standard value" (42) is used, or

$$C_6 \langle O_6 \rangle \simeq 0.05 \text{ GeV}^6, \quad (53)$$

if the value (45) is assumed. To remain on the safe side we have carried out the analysis allowing $C_6 \langle O_6 \rangle$ to vary in the generous range

$$-0.02 \text{ GeV}^6 \lesssim C_6 \langle O_6 \rangle \lesssim 0.2 \text{ GeV}^6. \quad (54)$$

A rough order of magnitude estimate of $C_6 \langle O_6 \rangle$ may be obtained by assuming vacuum

saturation /3.a/, i.e.

$$\langle (G_{\mu\nu} G_{\alpha\rho})^2 \rangle \simeq \frac{5}{16} \langle G^2 \rangle^2, \quad (55)$$

$$\langle (G_{\mu\alpha} G_{\nu\beta})^2 \rangle \simeq \frac{1}{16} \langle G^2 \rangle^2, \quad (56)$$

which yields

$$C_8 \langle O_8 \rangle \simeq (0.01 - 0.1) \text{ GeV}^8, \quad (57)$$

depending on which value of $\langle \alpha_s G^2 \rangle$ is used. Vacuum saturation, however, is not supported by any $1/N_c$ argument /26/ nor by specific instanton models /22/. Therefore, throughout our analysis we shall allow $C_8 \langle O_8 \rangle$ to depart from the value (57) by a generous order of magnitude.

3. B QCD-Sum Rules

Working with the second derivative of the function $\Pi_R(Q^2)/Q^2$, where $\Pi_R(Q^2)$ is given by (38), one easily finds the following Laplace-transform QCD-sum rule /3.a/

$$\begin{aligned} L(\sigma) &\equiv \int_0^\infty ds e^{-s\sigma} \frac{1}{\pi} \frac{\text{Im} \Pi(s)}{s} \\ &= \frac{C_0}{\sigma^2} + \Pi(0) - C_4 \langle O_4 \rangle - \frac{1}{2} C_6 \langle O_6 \rangle \sigma - \frac{1}{2} C_8 \langle O_8 \rangle \sigma^2. \end{aligned} \quad (58)$$

To estimate the resonance mass it is useful to consider the ratio

$$\frac{L'(\sigma)}{L(\sigma)} = \frac{\int_0^\infty ds e^{-s\sigma} \text{Im} \Pi(s)}{\int_0^\infty \frac{ds}{s} e^{-s\sigma} \text{Im} \Pi(s)}$$

$$= \frac{2c_0/\sigma^3 + c_6 \langle 0_6 \rangle + c_8 \langle 0_8 \rangle \sigma + \dots}{c_0^2 + \Pi(0) - c_4 \langle 0_4 \rangle - c_6 \langle 0_6 \rangle \sigma + \dots} \quad (59)$$

The Gaussian transform, needed to perform the heat evolution tests, is given

by

$$\begin{aligned} G(\hat{s}, \tau) &= \frac{1}{\sqrt{4\pi\tau}} \int_0^\infty ds \exp\left[-\frac{(s-\hat{s})^2}{4\tau}\right] \frac{\text{Im} \Pi(s)}{s} \\ &= c_0 \sqrt{\tau} \left[\frac{e^{-\hat{x}^2}}{\sqrt{\tau}} + \frac{1}{2} H_1(\hat{x}) H_1(\hat{x}) \text{Erfc}(-\hat{x}) \right] \\ &\quad + [\Pi(0) - c_4 \langle 0_4 \rangle] \frac{e^{-\hat{x}^2}}{2\sqrt{\pi\tau}} H_0(\hat{x}) \\ &\quad + c_6 \langle 0_6 \rangle \frac{e^{-\hat{x}^2}}{4\tau\sqrt{\tau}} H_4(\hat{x}) \\ &\quad - \frac{1}{2} c_8 \langle 0_8 \rangle \frac{e^{-\hat{x}^2}}{8\tau^{3/2}\sqrt{\tau}} H_2(\hat{x}) + \dots, \end{aligned} \quad (60)$$

where $\hat{x} \equiv \hat{s}/2\sqrt{\tau}$, $H_n(\hat{x})$ are Hermite polynomials, and

$$\text{Erfc}(x) = \frac{2}{\sqrt{\pi}} \int_x^\infty dy e^{-y^2} = 1 - \text{erf}(x), \quad (61)$$

Finally, the FESR in this channel are given by (28)-(30).

3.C Hadronic Spectral Function

Quark contributions, neglected in the QCD expression for $\Pi(Q^2)$, can be effectively taken into account in the spectral function by computing the scalar glueball coupling to $\pi\pi$, $K\bar{K}$, $\eta\eta$, ... intermediate states. Up to $S \approx 1 \text{ GeV}^2$ the $\pi\pi$ contribution is expected to dominate; a simple calculation gives

$$\frac{1}{\pi} \text{Im} \Pi(s) \Big|_{\pi\pi} = \frac{3}{2\pi^2} |F(s)|^2 \theta(s) \quad (62)$$

where

$$\begin{aligned} F(s) &\equiv \frac{1}{4} \langle 0 | \int | \pi(k_1) \pi(k_2) \rangle, \\ &\quad (k_1 + k_2)^2 \equiv s, \end{aligned} \quad (63)$$

and we have set $\mu_\pi^2 = 0$. Using the chiral Lagrangian realization of QCD at long distances it is possible to obtain the following low energy theorem /27/

$$F(s) \underset{s \rightarrow 0}{\sim} S \quad (64)$$

valid in the chiral $SU(2) \times SU(2)$ limit. Using this result to normalize a finite-

width parametrization of the spectral function we can write

$$\frac{1}{\pi} \text{Im} \Pi(s) \Big|_{\pi\pi} = \frac{3}{2\pi^2} s^2 \frac{M^4 (1 + \Gamma^2/M^2)}{(s-M^2)^2 + M^2 \Gamma^2} \quad (65)$$

In order to probe energy regions above 1 GeV we can improve (65) by adding the $K\bar{K}$ and $\eta\eta$ intermediate state contributions. From the flavour independence of $J(x)$ one may safely assume that the transition form factor analogous to (63) remains the same, in which case one has

$$\frac{1}{\pi} \text{Im} \Pi(s) = \frac{3}{2\pi^2} s^2 \frac{M^4 (1 + \Gamma^2/M^2)}{(s-M^2)^2 + M^2 \Gamma^2} \left[\theta(s) + \frac{5}{3} \sqrt{1 - 4M^2/s} \theta(s - 4f^2) \right], \quad (66)$$

where we have taken into account kinematical corrections to the chiral limit in the $K\bar{K}$ and $\eta\eta$ threshold for which we use the average value

$$4\mu^2 \simeq 1.09 \text{ GeV}^2. \quad (67)$$

It is possible to check that dynamical corrections to $F(s)$, which are of the form $f(1 + \mu^2/s)$, have a small impact on the results of our analysis.

3.0 Approximate Results

Before discussing detailed predictions for the 0^{++} glueball mass and width I wish to justify at this point the approximate results (4) and (6) quoted in Section 1. If the glueball mass lies below the threshold (67) and its width is small then to a good approximation one can neglect $K\bar{K}$ and $\eta\eta$ intermediate states and work with the spectral function (65). In narrow width (65) reduces to

$$\frac{1}{\pi} \text{Im} \Pi(s) \Big|_{\pi\pi}^{(0)} \simeq \frac{3}{2\pi} s^2 \frac{M^3}{\Gamma} \delta(s - M^2). \quad (68)$$

Using this approximate spectral function in the ratio of FESR (31) one obtains

$$M_{0^{++}}^2 \simeq \frac{C_0 S_0^3/3 + C_6 \langle 0_6 \rangle}{C_0 S_0^3/2 + \bar{\Pi}(0) - C_4 \langle 0_4 \rangle} \quad (69)$$

An inspection of the numerical values of the various terms in the r.h.s. of (69) (see (41), (43), (44), (45) and (54)) shows that $\bar{\Pi}(0) \gg C_4 \langle 0_4 \rangle$ and that, for $S_0 \simeq 1 - 3 \text{ GeV}^2$ where we expect duality to hold, the perturbative piece can be safely neglected in the denominator of (69). Its contribution in the numerator of (69) can be comparable to $C_6 \langle 0_6 \rangle$ and thus Eq. (4) is valid within a factor of two. The approximate formula for the total width (6) follows after substituting (68) in the first FESR (28) and neglecting $C_4 \langle 0_4 \rangle$ and the perturbative term in comparison to $\bar{\Pi}(0)$. Alternatively, using the ratio of Laplace transforms (59) and the same approximations as above one finds again Eq. (4) provided the continuum is neglected and $\sigma \simeq 0.5 - 1 \text{ GeV}^{-2}$. Although this continuum is suppressed relative to the resonance piece by a factor $e^{-s_0 \sigma}$ times the width Γ , its contribution may be important and the derivation of Eq. (4) may not be as transparent as with FESR. However, the complete analysis (see 3.6 below) shows that the eigenvalue solutions to the FESR are also solutions to the Laplace transform sum rules.

3.E Eigenvalue solutions to the FESR

The approximate estimates given in (4) and (6) and justified above may not be enough as they do not exclude possible 0^{++} excitations. The FESR (28)-(30) are the ideal tool to study this possibility as they weigh high energies. Sta-

bility tests based on e.g. the ratio (31) will tell us in the end whether or not the single resonance spectral function (66) saturates the hadronic integrals.

Tables 1 and 2 show some of the eigenvalue solutions to the FESR (28) - (30) corresponding to the standard value of the gluon condensate (42) and to the value (45), respectively. For a given value of $C_6 \langle 0_g \rangle$ one could find eigenvalue solutions with larger masses and widths but they would imply unreasonable high values of $C_9 \langle 0_g \rangle$. Notice that the last entry in each group is already implying a $C_9 \langle 0_g \rangle$ which exceeds the factorization estimate (57) by roughly a factor of 20 - 30 in Table 1, and by a factor of 10 - 20 in Table 2.

TABLE 1

$C_6 \langle 0_g \rangle$ (GeV ³)	Γ (MeV)	M (MeV)	γ_0 (GeV ³)	$C_9 \langle 0_g \rangle$ (GeV ³)
-0.02	1	282	1.88	0.12
	5	392	2.33	0.26
0.019	1	280	1.52	0.05
	5	391	2.10	0.16
	10	452	2.42	0.27
0.1	5	385	1.23	0.001
	10	447	1.87	0.07
	20	519	2.43	0.21
0.2	20	508	1.20	-0.05
	30	559	2.15	0.04
	50	630	2.92	0.28

Typical results for the ratio (31) are shown in Figs. 6 and 7. The solid curve corresponds to the hadronic r.h.s. of (31) computed with the spectral function (66) using M and Γ eigenvalue solutions to the FESR. The vertical lines are the QCD l.h.s. of (31) for $C_4 \langle 0_g \rangle$ and $\Pi(0)$ as in Eqs. (43)-(44), and $C_6 \langle 0_g \rangle = -0.0016 \text{ GeV}^3$ (crosses), 0.019 GeV^3 (dots), and 0.2 GeV^3 (horizontal bars). It should be clear from these figures that the eigenvalue problem is re-

TABLE 2

$C_6 \langle 0_g \rangle$ (GeV ³)	Γ (MeV)	M (MeV)	γ_0 (GeV ³)	$C_9 \langle 0_g \rangle$ (GeV ³)
-0.06	1	330	3.04	0.81
	5	468	3.82	1.86
0.06	1	349	2.64	0.45
	5	486	3.57	1.37
0.3	5	483	2.90	0.50
	10	559	3.60	1.19
0.6	10	553	2.57	0.08
	20	643	3.77	1.04

markably stable, i.e. there is a wide "duality region" for $1 \text{ GeV}^2 \lesssim S_0 \lesssim 3 \text{ GeV}^2$ which leaves no room for additional resonances.

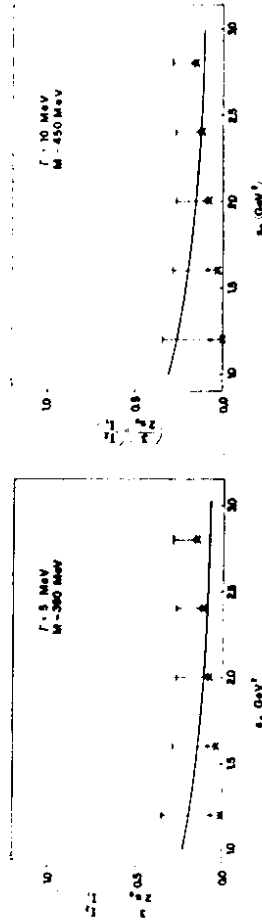


Fig. 6

Fig. 7

At this point it is possible to turn the problem around and ask for the implications of a heavy, $M \simeq 1 - 1.5 \text{ GeV}$, and broad, $\Gamma \simeq M/2$, scalar glueball. The behaviour of the r.h.s. of (31) computed with the spectral function (66) using $M = 1 \text{ GeV}$, $\Gamma = M/2$ as input is shown in Fig. 8 (curve a). Such a

heavy glueball would require $C_g \langle 0_g \rangle$ and $C_g \langle 0_g \rangle$ to be 50 times and -100 times bigger than the standard values, respectively. This is clearly well outside reasonable limits. Figure 8 also shows the behaviour of a "non-resonant" spectral function (curve b) obtained by simple extrapolation of the low energy behaviour, formally equivalent to the $M \rightarrow \infty$ limit in (66).

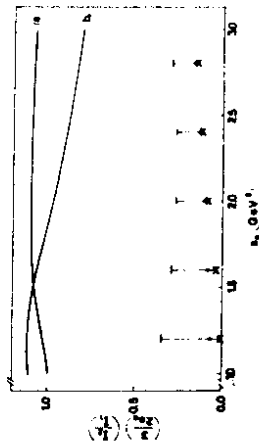


Fig. 8

3.F Heat evolution tests

The next step is to check quantitatively whether or not there is duality between the input values of the gluon condensates and the resonance parameters obtained as eigenvalue solutions to the FESR. This may be performed through the heat evolution test of BLR /20/ described in Section 2. It will also be useful to compare these results with those for a heavy and broad glueball.

Figures 9 - 11 show the "time" evolution of the heat distribution (25) computed with (66) using a typical eigenvalue solution from Table 1, viz $M = 452$ MeV, $\Gamma = 10$ MeV (dashed curves) and computed in QCD using the corresponding values of the condensates (solid curves). For "times" $\tau \gtrsim 1$ GeV⁴ there is nice agreement

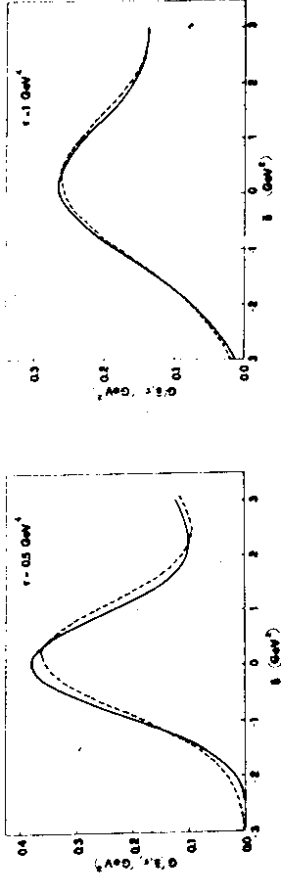


Fig. 9

Fig. 10

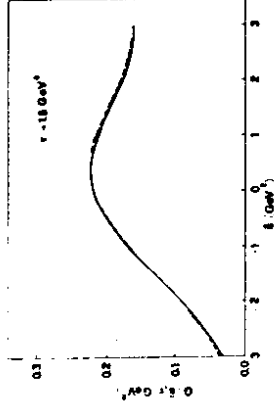


Fig. 11

between the hadronic and the QCD heat distributions in the semiinfinite rod $0 \leq \hat{s} < \infty$, indicating that duality is well satisfied. Such is not the case, though, for the $M = 1$ GeV, $\Gamma = 700$ MeV glueball found in /3.6/ from a Laplace transform analysis. In fact, Fig. 12 shows the heat distributions at $\tau = 1$ GeV⁴ computed with the same spectral function and for the same values of the condensates used in /3.b/. The rather pronounced disagreement between QCD and phenomenology observed in Fig. 12 is found to persist even for larger values of τ , and to become even more pronounced with increasing glueball mass. This is a good example illustrating that solutions to Laplace sum rules do not necessarily obey duality.

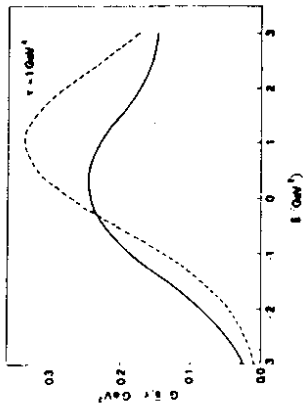


Fig. 12

3.G Laplace transform analysis

As shown above, the heavy and broad scalar glueball found in /3.b/ from Laplace sum rules does not show up in the FESR and does not pass the heat evolution tests. In order to try to understand the reason we have computed the Laplace transform (58) using our spectral function (66). The behaviour of $L(\sigma)$ versus σ is shown in Fig. 13 for $\Gamma = 10$ MeV and $M = 500$ MeV (curve a), $M = 452$ MeV (curve b),

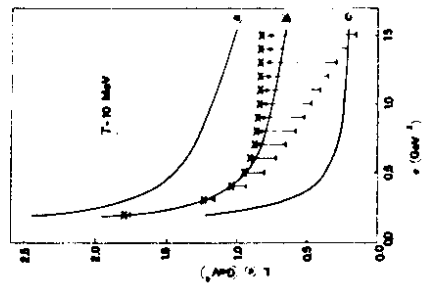


Fig. 13

and $M = 350$ MeV (curve c). The vertical lines are the Laplace transforms of the QCD expression, the r.h.s. of (58), for the same values of the condensates as in Figs. 6 - 7. Notice the remarkable agreement between both sides of (58), within the very wide window $0.2 \text{ GeV}^2 \leq \sigma \leq 1.5 \text{ GeV}^2$, for the true eigenvalue solution to the FESR (curve b). In contrast, as shown in Fig. 14, the hadronic l.h.s.

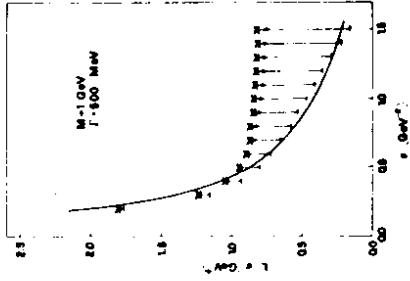


Fig. 14

of (58) for $M = 1$ GeV, $\Gamma = 500$ MeV coincides with the QCD r.h.s. only in a very narrow region around $\sigma \approx 0.5 \text{ GeV}^2$ where continuum effects are important. Since FESR are much more sensitive to S_0 , and thus more selective, this "Laplace-unstable" solution does not appear in FESR; it is simply not dual to QCD.

4. TENSOR GLUONIUM

4.A The two-point function $\Pi(Q^2)$ in QCD

Using the current (3) in (1) we can write

$$\begin{aligned} \Pi_{\mu\nu; \alpha\beta}(Q^2) &= i \int d^4x e^{iqx} \langle 0 | T(\theta_{\mu\nu}(x) \theta_{\alpha\beta}(0)) | 0 \rangle \\ &= \eta_{\mu\nu; \alpha\beta} T(Q^2), \end{aligned} \tag{70}$$

where $\gamma_{\mu\nu, \alpha\beta}$ is the spin-2 projector

$$\gamma_{\mu\nu, \alpha\beta} = \gamma_{\mu\alpha} \gamma_{\nu\beta} + \gamma_{\mu\beta} \gamma_{\nu\alpha} - \frac{2}{3} \gamma_{\mu\nu} \gamma_{\alpha\beta} \quad (71)$$

with

$$\gamma_{\mu\nu} = -g_{\mu\nu} + \frac{q_\mu q_\nu}{q^2} \quad (72)$$

The QCD expression for $\Gamma(Q^2)$ to lowest order in α_s and including the leading power corrections is given by /3.a/

$$\Gamma(Q^2) = C_0 Q^4 \ln v^2/\Lambda^2 + \frac{C_2 \langle O_2 \rangle}{Q^4} + \frac{C_0 \langle O_0 \rangle}{Q^6} + \dots \quad (73)$$

where

$$C_0 = 1 / (20 \pi^2), \quad (74)$$

$$C_2 \langle O_2 \rangle = \frac{5\pi}{3} \alpha_s \langle 2O_1 - O_2 \rangle, \quad (75)$$

and

$$O_1 \equiv (f^{abc} G_{\mu\alpha}^b G_{\nu\alpha}^c)^2, \quad (76)$$

$$O_2 \equiv (f^{abc} G_{\mu\nu}^b G_{\mu\nu}^c)^2. \quad (77)$$

Although the dimension - 10 gluon condensate in (73) is unknown we have included it for reasons that will become clear later. As in the case of scalar gluonium, an order of magnitude estimate of $C_0 \langle O_0 \rangle$ may be obtained by invoking vacuum

saturation. In such a case one finds

$$C_0 \langle O_0 \rangle \Big|_{\text{FACT}} \simeq -0.0046 \text{ GeV}^8, \quad (78)$$

if the standard value (42) of $\langle \alpha_s G^2 \rangle$ is used, or

$$C_0 \langle O_0 \rangle \Big|_{\text{FACT}} \simeq -0.041 \text{ GeV}^8, \quad (79)$$

for the value (45). Notice the asymptotic behaviour

$$\frac{1}{\pi} \text{Im} \Gamma(Q^2) \sim C_0 Q^4 \quad (80)$$

which calls for three subtractions in the dispersion relation.

4.8 QCD-sum rules

Working with the third derivative of $\Gamma(Q^2)$ in order to get rid of the three unknown subtraction constants one easily finds the following Laplace transform sum rules

$$L(\sigma) \equiv \int_0^\infty ds e^{-s\sigma} \frac{1}{\pi} \text{Im} \Gamma(s) = \frac{2C_0}{\sigma^3} + C_2 \langle O_2 \rangle \sigma - C_0 \langle O_0 \rangle \frac{\sigma^2}{2} + \dots \quad (81)$$

The Gauss-Weierstrass transform needed for the heat evolution tests is

$$\begin{aligned} G(\hat{s}, \tau) \Big|_{\text{QCD}} &= C_0 \tau \left[\frac{1}{\sqrt{\tau}} H_1(\hat{x}) e^{-\hat{x}^2} + \frac{1}{2} \text{Erfc}(-\hat{x}) \right. \\ &\quad \times \left. [4H_0(\hat{x}) + H_2(\hat{x})] \right] - \frac{C_2 \langle O_2 \rangle}{4\tau\sqrt{\pi}} H_1(\hat{x}) e^{-\hat{x}^2} \\ &\quad + \frac{C_0 \langle O_0 \rangle}{16\sqrt{\pi} \tau^{3/2}} H_2(\hat{x}) e^{-\hat{x}^2} + \dots \end{aligned} \quad (82)$$

Finally, the FESR in this channel read

$$c_0 \frac{s_0^3}{3} = \int_0^{s_0} ds \frac{1}{\pi} \text{Im} T(s), \quad (83)$$

$$c_0 \frac{s_0^4}{4} - c_8 \langle 0g \rangle = \int_0^{s_0} ds s \frac{1}{\pi} \text{Im} T(s), \quad (84)$$

$$c_0 \frac{s_0^5}{5} + c_{10} \langle 0_{10} \rangle = \int_0^{s_0} ds s^2 \frac{1}{\pi} \text{Im} T(s). \quad (85)$$

4.C Hadronic spectral function

The lowest intermediate state contribution to the spectral function is again the $\pi\pi$ state. We must consider then the matrix element

$$T_{\mu\nu} \equiv \langle \pi(p_1) \pi(p_2) | \Theta_{\mu\nu} | 0 \rangle = A \gamma_\mu \gamma_\nu + B q_\mu q_\nu + C g_{\mu\nu} + D (\gamma_\mu q_\nu + \gamma_\nu q_\mu), \quad (86)$$

where $r = p_1 = p_2$ and $q = p_1 + p_2$. The functions A, B, C, D can be related to each other by working in the chiral limit $p_1^2 = p_2^2 = \mu_\pi^2 = 0$ and imposing on (86) the following constraints: (a) transversality: $q^\mu T_{\mu\nu} = q^\nu T_{\mu\nu} = 0$; (b) tracelessness (to order α_s^0): $\langle \pi\pi | \Theta_{\mu}^{\mu} | 0 \rangle = 0(\alpha_s) \approx 0$; (c) crossed channel behaviour:

$$\langle \pi(p_1) | \Theta_{\mu\nu} | \pi(p_2) \rangle \xrightarrow{p_1 = p_2 = p} 2 p_\mu p_\nu \rho_G,$$

where ρ_G has been interpreted /27/ as the share of the pion momentum by the gluons ($\rho_G \leq 1$). Notice that in the scalar glueball case $\rho_G = 1$. In the present case, though, ρ_G must be considered as a free normalization parameter subject to the constraint $\rho_G \leq 1$; its value will have to be obtained from the sum rules together with the 2^{++} glueball mass and width. Using the constraints (a)-(c) above in (86) and computing the spectral function we obtain in the chiral limit

$$\frac{1}{\pi} \text{Im} T(s) = \frac{\rho_G^2}{640\pi^2} s^2 \frac{M^4 (1 + \Gamma^2/M^2)}{(s-M^2)^2 + M^2 \Gamma^2} \Theta(s). \quad (87)$$

Including $K\bar{K}$ and $\eta\eta$ intermediate state contributions, the simplest generalization of (87), which accounts for the flavour independence of the source $\Theta_{\mu\nu}$, may be written as

$$\frac{1}{\pi} \text{Im} T(s) = \frac{\rho_G^2}{640\pi^2} s^2 \frac{M^4 (1 + \Gamma^2/M^2)}{(s-M^2)^2 + M^2 \Gamma^2} \left[\Theta(s) + \frac{5}{8} (1 - 4\frac{F^2}{B})^{5/2} \Theta(s-4F^2) \right] \quad (88)$$

where $4\mu^2 \approx 1.09 \text{ GeV}^2$ is the average $K\bar{K}$ and $\eta\eta$ threshold.

4.D Solutions to the FESR

In order to predict M and Γ we have at our disposal the three FESR (83)-(85). However, s_0 , ρ_G and $c_{10} \langle 0_{10} \rangle$ are also part of the unknowns. Therefore, we choose the following strategy: we tentatively set $c_{10} \langle 0_{10} \rangle = 0$, input a value for the width Γ and solve the FESR to find M, s_0 and ρ_G . Since ρ_G increases with increasing Γ we stop the procedure whenever ρ_G exceeds its bound $\rho_G \leq 1$. The eigenvalue solutions obtained in this way are shown in Tables 3 and 4 for

TABLE 3

Γ (MeV)	M (MeV)	s_0 (GeV ²)	ρ_0
100	1.610	3.422	0.733
150	1.624	3.510	0.927
200	1.636	3.592	1.10

TABLE 4

Γ (MeV)	M (MeV)	s_0 (GeV ²)	ρ_0
100	2.109	5.842	0.629
150	2.122	5.956	0.791
200	2.135	6.070	0.935
250	2.148	6.179	1.070

the choices (79) and (80), respectively. It may be seen from these results that depending on the value of $C_g < 0_g >$ one can easily accommodate either the $\Theta(1710)$ or the $g_1(2050)$, two of the tensor glueball candidates. However, the eigenvalue problem turns out to be unstable, as seen from Fig. 15 where we have plotted the ratio of FESR

$$1 - \frac{4 C_g < 0_g >}{C_0 S_0^4} = \left(\frac{4}{3 S_0} \right) \frac{I_3(S_0, M, \Gamma)}{I_2(S_0, M, \Gamma)}$$

$$\equiv \left(\frac{4}{3 S_0} \right) \frac{\int_0^{S_0} ds s \operatorname{Im} T(s)}{\int_0^{S_0} ds \operatorname{Im} T(s)} \quad (89)$$

In fact, the QCD l.h.s. of (89) (solid curve) intercepts the hadronic r.h.s. (dashed curve) only at a single point. There is no "duality region", indicating

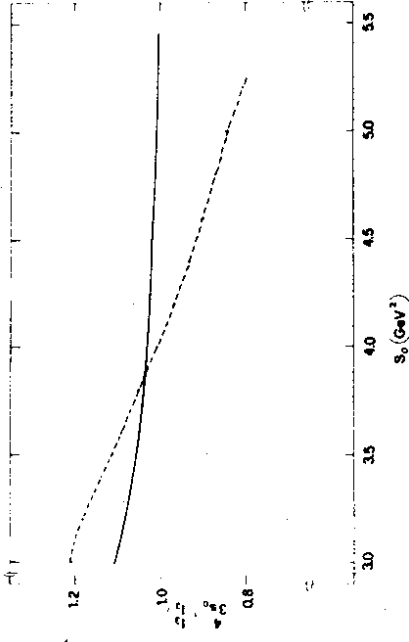


Fig. 15

that more hadronic information is needed in the spectral function around $S_0 \approx 4 \text{ GeV}^2$.

An obvious solution to the above instability problem may be to add a second resonance to $\rho(s)$, Eq. (88). A simple, albeit not unique, generalization of Eq. (88) is

$$\rho(s) \equiv \frac{1}{\pi} \operatorname{Im} T(s) = \frac{\rho_0^2}{640 \pi^2} s^2 \left[\theta(s) \right. \\ \left. + \frac{5}{8} \left(1 - 4 \frac{f^2}{s} \right)^{5/2} \theta(s - 4 f^2) \right] \times \left[\frac{M_1^4 (1 + \Gamma_1^2 / M_1^2)}{(s - M_1^2)^2 + M_1^2 \Gamma_1^2} \right. \\ \left. + \lambda \frac{M_2^4 (1 + \Gamma_2^2 / M_2^2)}{(s - M_2^2)^2 + M_2^2 \Gamma_2^2} \right] \quad (90)$$

where λ is a free parameter. In spite of Eq. (90) being the most economical generalization of Eq. (88), the number of unknown hadronic parameters has become too large. With only three FESR at our disposal it is clear that the analysis is bound to be only semi-quantitative. Nevertheless, we can study the consistency between a given set of input values for the mass and width of the two resonances and the resulting values of ρ_G , $C_g \langle 0_g \rangle$, and $C_{10} \langle 0_{10} \rangle$ obtained by solving the FESR. By adjusting the parameter λ we can see whether a reasonably wide duality window now exists for the ratio (89) as well as for ρ_G , $C_g \langle 0_g \rangle$ and $C_{10} \langle 0_{10} \rangle$. These parameters should not only be stable against changes in s_0 but also their values should not differ much from those of the single resonance analysis. Following this strategy we have found that using the Θ (1710) and $g_T(2050)$ parameter it is indeed possible to achieve a remarkable overall stability, to wit. In Fig. 16 we show the ratio (89) as a function of s_0 for $\lambda = 0.5$. The

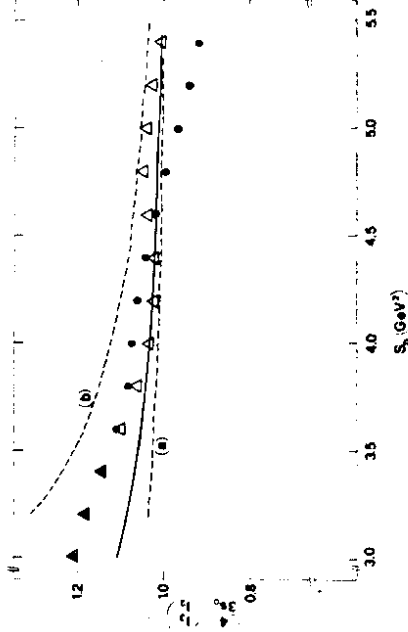


Fig. 16

triangles correspond to the hadronic right-hand side of Eq. (89) with $M_1 = 1.71$ GeV, $\Gamma_1 = 150$ MeV, $M_2 = 2.15$ GeV and $\Gamma_2 = 200$ MeV, while the closed circles correspond to the same M_1 , Γ_1 but $M_2 = 2$ GeV, and $\Gamma_2 = 200$ MeV. The solid curve corresponds to the QCD-left-hand side of Eq. (89) with $C_g \langle 0_g \rangle = -0.0115$ GeV⁸ and the broken curves (a) and (b) are calculated with

the two extreme choices $C_g \langle 0_g \rangle = -0.041$ GeV⁸ and $C_g \langle 0_g \rangle = -0.0046$ GeV⁸, respectively. Figures 17, 18 and 19 show the predictions for ρ_G , $C_g \langle 0_g \rangle$ and

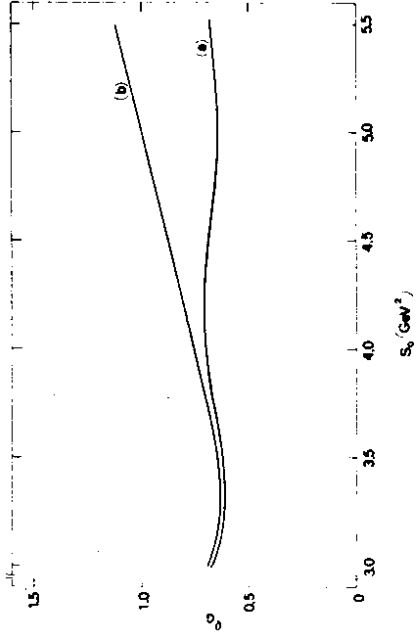


Fig. 17

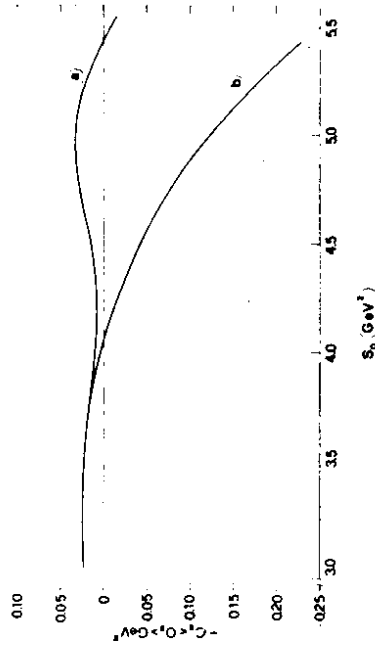


Fig. 18

$C_{10} \langle 0_{10} \rangle$, respectively, obtained by solving the FESR (83)-(85) with $\rho(s)$ given by Eq. (90) with $\lambda = 0.5$ and the Θ (1710) and $g_T(2050)$ parameters. For comparison we also show in Figs. 17-19 the corresponding predictions using the single resonance spectral function (88) with the Θ (1710) mass and width.

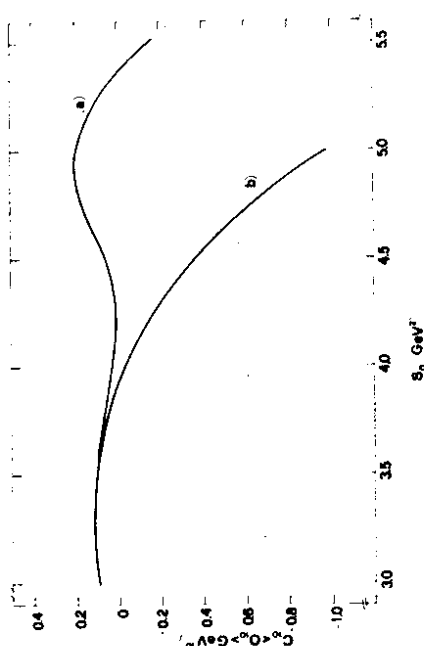


Fig. 19

A comparison of Fig. 16 with Fig. 15 shows quite clearly how the addition of a second resonance to $\rho(s)$ solves the stability problem. In fact, the two-resonance saturation of the spectral function leads to a wide duality window extending from $s_0 \approx 3 \text{ GeV}^2$ to $s_0 \approx 5.5 \text{ GeV}^2$. Furthermore, as seen from Figs. 17-19 the parameters C_4 , $C_8 \langle 0_8 \rangle$ and $C_{10} \langle 0_{10} \rangle$ become remarkably more stable after a second resonance is added to $\rho(s)$. We wish to reiterate, however, that given the approximations contained in Eq. (90) and given the number of unknown parameters, we cannot claim to have predicted the mass and width of the two glueballs. Our analysis only shows that if the $\theta(1710)$ and the $g_1(2050)$ were to be established experimentally as bonafide tensor glueballs, then their masses and widths would be compatible with QCD in a stable sense. However, our analysis of the stability of the eigenvalue solutions to the FESR has provided a strong hint that in addition to a ground state glueball with $M \approx 1.6 - 1.7 \text{ GeV}$, $\Gamma \approx 100 - 200 \text{ MeV}$, there should exist at least another resonance with $M \approx 2 \text{ GeV}$, $\Gamma \approx 200 \text{ MeV}$. In spite of being qualitative, we find this conclusion quite interesting by itself.

4.E Heat evolution tests

In order to check quantitatively whether or not there is duality between the hadronic parameters in (90) and the QCD information obtained from the FESR as described above, we have computed the Gaussian transforms (82) as a function of ξ and for various "times" τ . In Figs. 20-21 we show e.g. the behaviour of $U^{(+)}(\xi, \tau) = G(\xi, \tau) + G(-\xi, \tau)$ at $\tau = 0.5 \text{ GeV}^4$ and $\tau = 1.5 \text{ GeV}^4$. The time evolution of $G(\xi, \tau)$ or $U^{(-)}(\xi, \tau) = G(\xi, \tau) - G(-\xi, \tau)$ is equally good and provides the final test of our results.

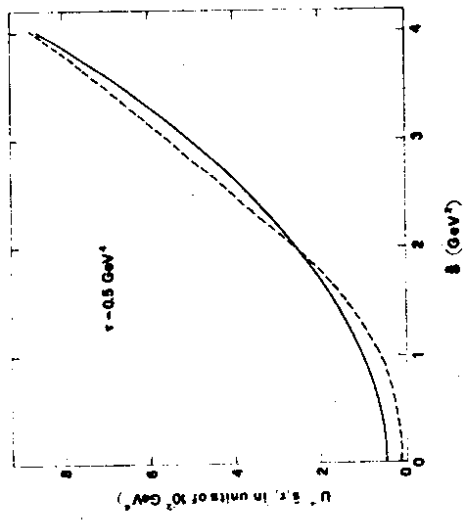


Fig. 20

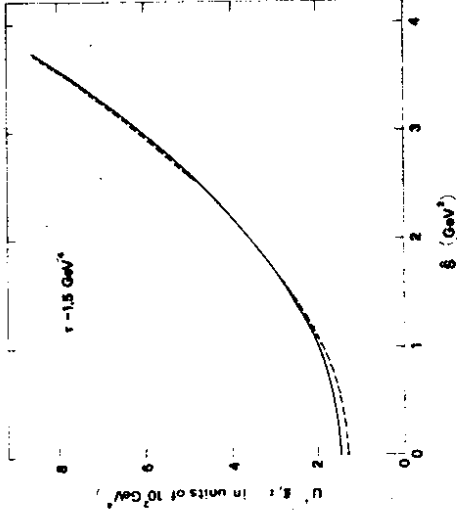


Fig. 21

REFERENCES

- /1/ H. Fritzsche, M. Gell-Mann, Proc. 16th International Conference on High Energy Physics, Vol. 2 (FNAL, Batavia, 1972); H. Fritzsche, P. Minkowski, Nuovo Cimento A30, 393 (1975)
- /2.a/ Ph. de Forcrand, G. Schierholz, M. Schneider, M. Teper, Phys. Lett. 152B, 107 (1985); Z. Phys. C - Particles and Fields 31, 87 (1986)
- /2.b/ A. Patel, R. Gupta, G. Guralnik, G.W. Kilcup, S.R. Sharpe, Univ. of California Report No. UCSD-10 P. 10 - 260 (1986)
- /2.c/ M. Teper, Proc. Workshop on Non Perturbative Methods, Ed. S. Narison (World Scientific, Singapore, 1985)
- /3.a/ V.A. Novikov, M.A. Shifman, A.I. Vainshtein, V.I. Zakharov, Nucl. Phys. B165, 67 (1980); B191, 301 (1981)
- /3.b/ P. Pascual, R. Tarrach, Phys. Lett. 113B, 495 (1982)
- /3.c/ S. Narison, Z. Phys. C - Particles and Fields 26, 209 (1984)
- /3.d/ C.A. Dominguez, N. Paver, Z. Phys. C - Particles and Fields 31, 591 (1986)
- /3.e/ C.A. Dominguez, N. Paver, Z. Phys. C - Particles and Fields 32, 391 (1986)
- /3.f/ N.V. Krashnikov, A.A. Pivovarov, N.N. Tavkhelidze, Z. Phys. C - Particles and Fields 19, 301 (1983)
- /4.a/ R.L. Jaffe, K. Johnson, Phys. Lett. 60B, 201 (1976)
- /4.b/ J.F. Donoghue, K. Johnson, B.A. Li, Phys. Lett. 99b, 416 (1981)
- /4.c/ T. Barnes, F.E. Close, S. Moneghan, Phys. Lett. 110B, 159 (1982)
- /4.d/ T.H. Hansson, K. Johnson, C. Peterson, Phys. Rev. D26, 2069 (1982)
- /4.e/ C.E. Carlson, T.H. Hansson, C. Peterson, Phys. Rev. D27, 1556 (1983)
- /4.f/ M. Chanowitz, S.R. Sharpe, Nucl. Phys. 222B, 211 (1983)
- /4.g/ T. Barnes, F.E. Close, F. de Viron, Nucl. Phys. B224, 241 (1983)
- /5.a/ T. Barnes, Z. Phys. C - Particles and Fields 10, 275 (1981)
- /5.b/ J.M. Cornwall, A. Soni, Phys. Lett. 120B, 431 (1983)
- /5.c/ F. Caruso, A.F.S. Santoro, M.H.G. Souza, C.O. Escobar, Phys. Rev. D30, 69 (1984)
- /5.d/ J. Ellis, J. Lanik, Phys. Lett. 150B, 289 (1985)
- /5.e/ G.J. Gounaris, R. Kögerler, J.E. Paschalis, Nucl. Phys. B276, 629 (1986); Z. Phys. C - Particles and Fields 31, 277 (1986)
- /5.f/ H.G. Gomm, P. Jain, R. Johnson, J. Schechter, Phys. Rev. D33, 801 (1986)
- /6.a/ B. Berg, A. Billoire, C. Vohwinkel, Florida State University Report No. FSU-SCRI-86-06 (1986)
- /6.b/ R.V. Gavai, A. Gockasch, U.M. Heller, Univ. California, San Diego, Report No. UCSD-10P10-268 (1986)
- /7/ C.E. Carlson, J.J. Coyne, P.M. Fishbane, F. Gross, S. Meshkov, Phys. Lett. 99B, 353 (1981)
- /8/ D. Alde et al., Nucl. Phys. B269, 485 (1986)
- /9/ T. Akesson et al., Nucl. Phys. B264, 154 (1986)
- /10/ S.R. Sharpe, R.L. Jaffe, M.R. Pennington, Phys. Rev. D30, 1013 (1984)
- /11/ K.L. Au, D. Morgan, M.R. Pennington, Phys. Lett. 167B, 229 (1986); Rutherford Report No. RAL-86-076 (1986)
- /12/ For a description of these data see /11/
- /13.a/ C. Edwards et al., Phys. Rev. Lett. 48, 458 (1982)
- /13.b/ D.M. Coffmann et al., SLAC Report No. SLAC-PUB-3720 (1986)
- /14/ A. Etkin et al., Phys. Rev. Lett. 49, 1620 (1982)
- /15/ D. Bisello et al., Phys. Lett. 179B, 294 (1986)
- /16.a/ C.A. Heusch, SLAC Report No. SLAC-PUB 3556 (1985)
- /16.b/ S. Cooper, Proc. International Europhysics Conference on High Energy Physics, Eds. L. Nitti, E. Preparata (Bari, 1985)
- /17.a/ H.G. Dosch, Proc. Workshop on Non Perturbative Methods, Ed. S. Narison (World Scientific, Singapore, 1985)
- /17.b/ L.J. Reinders, H. Rubinstein, S. Yazaki, Phys. Rep. 127, 1 (1985)
- /18.a/ R.A. Bertlmann, C.A. Dominguez, M. Loewe, M. Parrottet, E. de Rafael, DESY Report (to appear)
- /18.b/ R.A. Bertlmann, Proc. XVII International Symposium on Multiparticle Dynamics, Seewinkel, Austria, June 1986 (to be published), and Univ. Wien Report No. UW Th. Ph. - 1986 - 25 (1986)
- /18.c/ C.A. Dominguez, invited talk at this Workshop
- /19/ M.A. Shifman, A.I. Vainshtein, V.I. Zakharov, Nucl. Phys. B147, 448, 519 (1978)
- /20.a/ R.A. Bertlmann, G. Launer, E. de Rafael, Nucl. Phys. B250, 61 (1985)
- /20.b/ G. Launer, Z. Phys. C - Particles and Fields 32 557 (1986)
- /21.a/ C.A. Dominguez, Z. Phys. C - Particles and Fields 26, 269 (1984)
- /21.b/ C.A. Dominguez, M. Kremer, N. Papadopoulos, K. Schilcher, Z. Phys. C - Particles and Fields 27, 481 (1985)

- /21.c/ C.A. Dominguez, M. Loewe, Phys. Rev. D31, 2930 (1985)
- /21.d/ A. Pich, E. de Rafeel, Phys. Lett. 158B, 477 (1985)
- /21.e/ C.A. Dominguez, E. de Rafeel, Ann. Phys. (N.Y.) to be published; Univ. Wien Report No. UW Th. Ph. - 1986 - 13 (1986)
- /22/ E.V. Shuryak, Nucl. Phys. B203, 93, 116, 140 (1982)
- /23.a/ S.N. Nikolaev, A.V. Radyushkin, Sov. J. Nucl. Phys. 39, 91 (1984)
- /23.b/ A.R. Zhitnitskii, Sov. J. Nucl. Phys. 41, 513 (1985)
- /24/ M. Müller -Preusser, Phys. Lett. 122B, 165 (1983)
- /25.a/ A. Di Giacomo, K. Fabricius, G. Paffuti, Phys. Lett. 118B, 129 (1982)
- /25.b/ A. Di Giacomo, Proc. Workshop on Non Perturbative Methods, Ed. S. Narison (World Scientific, Singapore, 1985)
- /26/ V.A. Novikov, M.A. Shifman, A.I. Vainshtein, V.I. Zakharov, Nucl. Phys. B237, 525 (1984)
- /27/ V.A. Novikov, M.A. Shifman, Z. Phys. C - Particles and Fields 8, 43 (1981)